

## FRINGE CODE REDUCTION FOR 3D MEASUREMENT SYSTEMS USING EPIPOLAR GEOMETRY

C. Bräuer-Burchardt, C. Munkelt, M. Heinze, P. Kühmstedt, G. Notni

Fraunhofer IOF Jena, Albert-Einstein-Str. 7, D-07745 Jena, Germany  
christian.braeuer-burchardt@iof.fraunhofer.de

Commission III, WG III/1

**KEY WORDS:** Fringe projection, Epipolar geometry, 3D measurements, Calibration, Image analysis

### ABSTRACT:

In this work a new approach for code reduction for fringe projection 3D measurement systems is introduced. These devices are used for contactless 3D surface measurement with high accuracy. In order to prevent ambiguities in the point correspondences usually Gray-Code sequences are used leading to long recording times. In our approach we use the restriction of the valid measuring volume and epipolar constraints to reduce the valid area for proper point correspondences. This reduces the necessary number of Gray-Code images in the sequence. The inclusion of the epipolar geometry of the projector leads to further reduction of images, and, if the arrangement is especially designed to unambiguously of the point correspondence excluding the Gray-Code at all. The projection of the fringes approximately perpendicular to the direction of the epipolar lines allows the omission of a second projection direction. First results show that both the completeness and the accuracy of the new method are comparable to the conventional technique. A considerable reduction of the number of recorded images and hence a speed-up of the image recording time can be achieved.

### 1. INTRODUCTION

Fringe projection is increasingly used to design contactless measuring systems for industrial, technical and medical applications. Whereas flexibility, measuring accuracy, measurement data volume, and fields of application always increase, the processing time should be reduced. New developments in computer technology help to satisfy these demands but new technologies and algorithms must be developed additionally. Recently, several measuring principles have been established in order to realize a contactless determination of the surface of measuring objects. Methods of photogrammetry are confronted to techniques using structured light. However, these principles have already been merged leading to methods called phasogrammetry or active stereo vision.

Battle (Battle et al., 2007) gives an extensive survey over coded structured light techniques to solve the correspondence problem which is the basis for 3D surface reconstruction. Coded structured light does not only include fringes but also other patterns. In our work, however, we use fringe patterns. Methods using the projection of sinusoidal fringe patterns have to solve the problem of phase unwrapping. This can be realized e.g. by the use of multiple spatial frequencies (Li et al., 2005), temporal phase unwrapping methods (Zhang et al., 1999), or the use of Gray-Code sequences (Sansoni et al., 1999). Because of the unambiguously the use of the Gray-Code leads to robust results. However, longer image sequences must be recorded which is not always desired.

In this work, our goal was to reduce the number of images of a structured light pattern sequence in order to speed-up the image recording time of fringe projection 3D-measurement systems. Additionally, fast applications (real-time applications or moving objects measurement) should become possible. Malz suggests in his work (Malz, 1989) a method of phase

unwrapping by projection of trapezoidal patterns. A method which projects dot grids of various increments onto the measuring object in combination with a simultaneous image recording by four cameras is described by Maas (Maas, 1992). The epipolar geometry information is used there to realize the point correspondences between the camera images.

Zhang suggests a real-time coordinate measurement (Zhang and Yau, 2006) where the phase unwrapping is realized by determination and tracking of a marker. An interesting method for phase unwrapping using at least two cameras is presented by Ishiyama (Ishiyama et al., 2007a). There the number of possible correspondences is drastically reduced by backpropagation of the correspondence candidates into the image of the second camera. Ishiyama gives another suggestion for 3D measurement using a one projector one camera fringe projection system (Ishiyama et al., 2007b) using the invariance of cross-ratio of perspective projection. Young (Young et al., 2007) suggests the use of the limitation of the measuring volume in order to reduce the search area for corresponding points on the epipolar line to segments. He achieves a reduction of the projected binary code by careful placement of additional cameras (or additional measuring positions). Li (Li et al. 2009) uses this approach together with the multi-frequency technique in order to realize real-time 3D measurements.

In this paper, a suggestion for phase unwrapping of single frequency fringe patterns with reduced Gray-Code sequences is given. This may be useful for applications where a short recording time of the image sequences is necessary. Such applications are for example reconstruction of living objects (e.g. face recognition) which can be without motion only for a short time and other measurement tasks which require real-time processing. Finally, a method to design systems is proposed where no Gray-Code at all is necessary for achieving uniqueness of the point correspondence.

## 2. MEASURING PRINCIPLES

### 2.1 Phasogrammetry

The classical approach of fringe projection is described e.g. by Schreiber (Schreiber and Notni, 2000) and can be briefly outlined as follows. A fringe projection unit projects some well defined fringe sequences for phase calculation onto the object, which is observed by a camera. Measurement values are the phase values  $\phi$  obtained by the analysis of the observed fringe pattern sequence at the image co-ordinates  $[x, y]$  of the camera. The 3D co-ordinates  $X, Y, Z$  of the measurement point  $M$  are calculated by triangulation, see e.g. (Luhmann et al., 2006). The calculated 3D co-ordinate directly depends (proportionality) on the phase value  $\phi$ .

### 2.2 Stereo Vision

Using the active stereo vision method, images of the object are captured from two different perspectives. Pairs of image co-ordinates  $[x_1, y_1]$  and  $[x_2, y_2]$  resulting from the same object point (the homologous points) have to be identified. On the basis of these points the object can be reconstructed using triangulation methods. The basic task is to identify the homologous points in both cameras. In the case of active stereo vision a single intensity pattern or a sequence of patterns are projected onto the object under measure.

To identify the homologous points in both cameras one has to use complex area (Robin and Valle, 2004) or image sequence based correlation techniques (Albrecht and Michaelis, 1997) using the captured intensity values. For example, the use of a sequence of statistical patterns was demonstrated for face scanning with the use of 20 patterns (Wiegmann et al., 2006). Commonly used area based correlation techniques are limited in the achievable precision caused by the deformation of the objects. Limits for this statistically correlation are the depth of field (considerable smaller compared to fringe projection) and the spatial resolution.

### 2.3 Point Correlation

The principle of phase correlation (Kühmstedt et al., 2007a) is to use the projected patterns only as virtual landmarks on the object to be measured and not for the data calculation itself. The basic hardware for a phase correlation system may consist of one fringe projector and two cameras C1 and C2. The projector generates two independent fringe sequences rotated by  $90^\circ$  to each other usually consisting of cosine and Gray-Code patterns. As a result we get two pairs of phase maps  $(\phi_{1,x}, \phi_{1,y})$  and  $(\phi_{2,x}, \phi_{2,y})$  at each object point  $M$  observed by the cameras from different perspectives. Normally, these phase maps should be unwrapped where mainly the Gray-Code technique is in use. These absolute phase maps can now be used for a point by point correlation between the images.

Starting from camera C1 with image co-ordinates  $[x_1, y_1]$  and phase values  $(\phi_{1,x}, \phi_{1,y})$  the corresponding image point in camera C2 is searched. Image co-ordinates  $[x_2, y_2]$  in camera C2 are calculated with sub-pixel accuracy, based on the identical phase information (phase values  $(\phi_{2,x}^{(corr)}, \phi_{2,y}^{(corr)}) = (\phi_{1,x}, \phi_{1,y})$ ). The final results of this correlation are pairs of image points resulting from the same object point - the homologous points. On the basis of the identified homologous points the calculation of the 3D co-ordinates is done by the well known triangulation technique.

The complete process of the measurement consists of data capturing and calculation. Data capturing usually includes the projection of two  $90^\circ$  rotated fringe sequences and the simultaneous image recording with both cameras. Data calculation contains the calculation of the phase maps for each camera, a point by point correlation of the phase maps between both cameras, the triangulation (co-ordinate calculation) between the homologous points in both cameras, and the 3D shape determination of the measured object.

## 3. EPIPOLAR CONSTRAINT

### 3.1 Epipolar Geometry

The epipolar geometry is a well known principle which is often used in photogrammetry when stereo systems are present. See for example (Luhmann et al., 2006). It is characterized by an arrangement of two cameras observing almost the same object scene. A measuring object point  $M$  defines together with the projection centres  $O_1$  and  $O_2$  of the cameras a plane  $E$  in the 3D space (see also Figure 1). The images of  $E$  are corresponding epipolar lines concerning  $M$ . When the image point  $m$  of  $M$  is selected in camera image I1 the corresponding point  $m_2$  in camera image I2 must lie on the corresponding epipolar line. This restricts the search area in the task of finding corresponding points.

In the following we assume a system consisting of two cameras C1 and C2 and one projector in a fix arrangement. The triangulation angle between the two cameras should be denoted by  $\tau_{C1C2}$ . Initially, the projector is arranged between the two cameras having a triangulation angle  $\tau_{C1P}$  to the cameras of about the half of  $\tau_{C1C2}$ .

### 3.2 Distortion of the Epipolar Lines

The distortion of the optical components of fringe projection systems must be considered for high precision measurements. Recently a number of works dealing with this subject have been published (Bräuer-Burchardt et al., 2005). Therefore we only refer to this subject but do not give any explanation. However, it must be realized that distortion leads to transformation of the straight lines into curves. Hence the epipolar lines become epipolar curves or, an image transformation according to the distortion, i.e. a distortion correction is performed. In the following we suppose that the distortion problem is solved and for easier handling we consider straight lines and line segments.

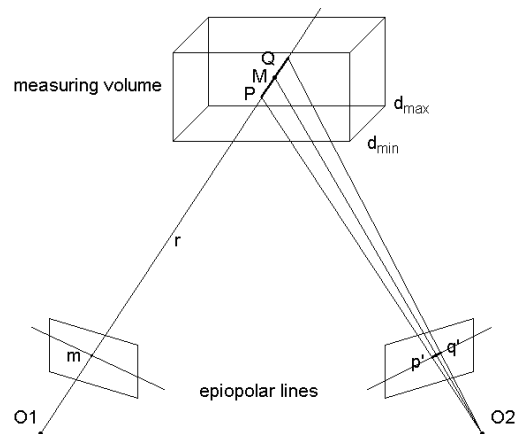


Figure 1: Measuring volume and epipolar segment  $p'q'$

### 3.3 Epipolar Segments

Fringe projection systems often operate in a well defined measuring volume. This is due to the geometric arrangement of the components and, additionally often restricted by the depth of focus. The triangulation angle  $\tau_{C1C2}$  between the cameras should be not too small because of the dependence of the measurement accuracy on  $\tau_{C1C2}$ . Hence, the part of the scene which is observed by both cameras is restricted lateral and in depth. Additionally, the objects to be measured are usually limited in size and position which also restricts the measuring volume. This leads to a typical situation as depicted in Figure 1.

Let us consider now the epipolar geometry. An image point  $p$  in camera C1 defines a visual ray  $r$  which is mapped into a straight line  $g$  in camera C2. However, the measuring volume restricts the part of  $r$  which contains the interested information into a section  $PQ$  of  $r$ . The image  $p'q'$  of  $PQ$  in camera C2 is a section again, namely a segment  $s$  of  $g$ . Because only points on  $s$  may have their origin in the valid measuring volume, the number of corresponding candidates to point  $p$  is reduced.

### 3.4 Epipolar Geometry and Fringe Projection

In fringe projection systems corresponding points can be uniquely identified by using a Gray-Code sequence. Thus phase information is unique and point correspondence is trivial, assuming no errors and artifacts in the phase images. Practical application would lead to a method using epipolar geometry and full Gray-Code sequence which should be denoted by **M1**.

However, our aim is the further reduction of the number of projected images. When the Gray-Code sequence is omitted, the point correspondence becomes ambiguous and this problem should be solved. Without using the Gray-Code we obtain a periodic rough phase image.

## 4. THE NEW APPROACH

### 4.1 Reduction of the Gray-Code Sequence

Consider now a point  $p$  in the camera C1 image and the resulting epipolar geometry. The point  $p$  defines an epipolar line  $g$  in image 2 and the valid measuring volume defines together with  $g$  a line segment  $s$ . The corresponding point  $p'$  must be on  $s$ . The actual phase value  $\phi$  of  $p$  resulting from camera image 1 defines the correspondence candidates for  $p'$  on  $s$  (see Figure 2). The number  $n$  of these candidates depends on the projected fringe width, the triangulation angle  $\tau_{C1C2}$  between C1 and C2, the measuring volume, and the shape of the measuring object. We have actually as many candidates as fringe periods cover the epipolar segment  $s$  (see Figure 2).

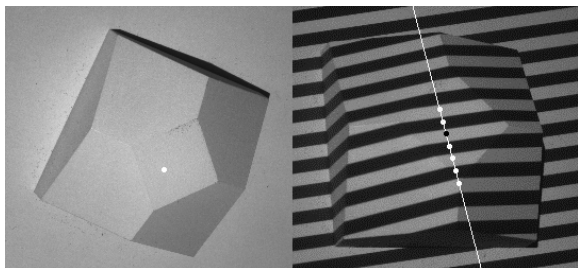


Figure 2: Images (sections) of C1 and C2 with selected point (left), epipolar line with candidates on epipolar segment (right)

One possibility to solve the correspondence problem is to add a reduced Gray-Code sequence depending on the maximal number  $n_{max}$  of candidates over the whole image area. The precise number of necessary Gray-Code images can be obtained by consideration of the shortest possible period length  $\lambda$  in the camera image and depends on the number of projected periods by the projector, the intrinsic and extrinsic orientation data of the cameras and the projector, and the measuring volume.

The calculation is performed by the following algorithm. First, the estimation of the shortest possible period length  $\lambda_{C2}^{min}$  of the fringe image in camera C2 according to formula (1) is performed:

$$\lambda_{C2}^{min} \approx \lambda_p \cdot \frac{c_{C2}}{c_p} - \tan \tau_{C2P} \cdot c_{C2} \frac{d_{max} - d_{min}}{d_{min}} \quad (1)$$

where  $c_{C2}$  = principal distance of camera C2  
 $c_p$  = principal distance of projector  
 $\lambda_p$  = fringe period length on the projector chip.  
 $\tau_{C2P}$  = triangulation angle between projector and C2  
 $d_{min}, d_{max}$  = minimal and maximal distance of the measuring volume concerning principal point  $p$ .

Figure 3 illustrates the geometric situation.

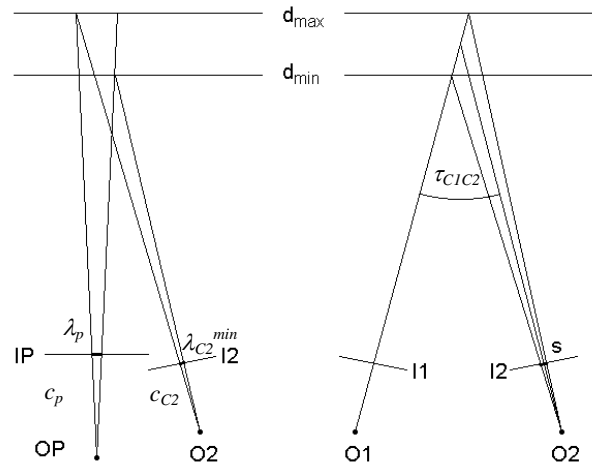


Figure 3: Shortest period length  $\lambda_{C2}^{min}$  (left) and segment length  $s$  for point  $p$  (right) according (1) and (2), view from above

The fringe period length on the projector chip  $\lambda_p$  is the product of the projector pixel size and the number of pixels (usually a power of 2) describing one period of the fringe pattern. Then for the principal point  $p$  of C1 the corresponding epipolar segment  $s$  in C2 is calculated. The length  $len(s)$  of  $s$  (illustrated by Figure 3) is obtained by

$$len(s) = c_{C2} \cdot \left( \frac{d_0 - d_{min}}{d_{min}} + \frac{d_{max} - d_0}{d_{max}} \right) \cdot \tan \tau_{C1C2} \quad (2)$$

where  $\tau_{C1C2}$  = triangulation angle between C1 and C2  
 $d_0$  = focal distance

The length  $len(s_i)$  of a segment  $s_i$  belonging to an arbitrary point  $p_i$  may slightly differ from  $len(s)$  and should be estimated considering the actual geometry of the system. The necessary number  $m_i$  of periods for a point  $p_i$  is obtained by

$$m_i = \frac{\text{len}(s_i)}{\lambda} \quad (3)$$

The maximum  $m$  of all  $m_i$  determines now the necessary number  $n$  of binary code images by the inequality

$$2^{n-1} < m \leq 2^n. \quad (4)$$

It should be noted that using the over-determined Gray-Code one more image is necessary than the calculated  $n$ . As we could see in our experiments, an adequate reduction of the Gray-Code sequence does not influence the completeness and correctness of the measurement at all.

Additionally, there arises a second option for a possible further reduction of the Gray-Code sequence which should be described here. As a third component, the orientation data of the projector is additionally included. Typically, the projector is symmetrically arranged between the two cameras. Hence there is a triangulation angle between the projector and one camera of about  $\tau_{C1C2} / 2$ . Considering now the epipolar segment of an image point in the projector image, it contains typically about the half number of projected periods. Consequently, the necessary length of the Gray-Code sequence remains constant or can be decreased by one additional image. The method arising from these remarks should be denoted by **M2**.

#### 4.2 Omission of the Gray-Code Sequence

Now, an approach for the total omission of the Gray-Code sequence will be given. Lets start with a fixed point  $p = (x,y)$  in the C1 image and searching for the corresponding point  $p'$  in the C2 image. Let the phase value be  $\phi$  at the position  $p$ . As shown in section 4.1 a number of  $n$  candidates  $p'_1, \dots, p'_n$  are yielded by phase correlation on the epipolar segment in C2. For every candidate  $p'_i$  we may now calculate the 3D co-ordinate by backpropagation and obtain  $P_i=(X_i,Y_i,Z_i)$ . Using the calibration data of the projector, every  $P_i$  leads to a corresponding phase value  $\phi_i$ . This value can be compared to the phase value  $\phi$  from the phase image of C1 at position  $p$ . Now, using a meaningful threshold  $thr$ , a number of candidates of the  $p'_i$  drop out. In order to obtain uniqueness we now have several opportunities denoted by M3, M4, and M5.

##### Method M3

First, we could select that candidate having the smallest distance in the phase value. This is unique but depending on the geometry of the measuring object a number of correspondence errors (see section 5) will be made.

##### Method M4

Second, instead of using the Gray-Code one can use a second projection direction perpendicular to the first one as in conventional systems. Using the algorithm we proposed before (Bräuer-Burchardt et al., 2008) together with the epipolar segments, the remaining ambiguities of the point correspondences are almost completely prevented.

##### Method M5

Finally, unambiguousness may be enforced by a third method. However, this method requires a certain arrangement of the geometric configuration, namely the relative orientation between the projector and the first camera. This will be achieved by a small triangulation angle  $\tau_{C1P}$  between the

projector and the camera C1. Hence, epipolar segments of no longer than one period in the projector image are produced. Hence, the absolute phase is known and backpropagation to C2 image identifies the correct corresponding candidate. The necessary triangulation angle  $\tau_{C1P}$  is approximately obtained by reformulating formula (2) substituting C2 by P and setting the period length  $\lambda_p$  of one fringe on the projector chip for the length of the epipolar segment  $s$

$$\tau_{C1P} = \arctan \left( \frac{\lambda_p}{c_p \cdot \left( \frac{d_0 - d_{\min}}{d_{\min}} + \frac{d_{\max} - d_0}{d_{\max}} \right)} \right). \quad (5)$$

Additionally, the position of  $s$  in the projector image defines the absolute unwrapped phase value for  $\phi$ . The situation is shown by Figure 4. For practical application two major issues should be considered. First, it should be sure that the selected distance range  $[d_{\min}, d_{\max}]$  of the measuring volume is sufficient. Second, the mechanic realization of the resulting triangulation angle  $\tau_{C1P}$  must be ensured.

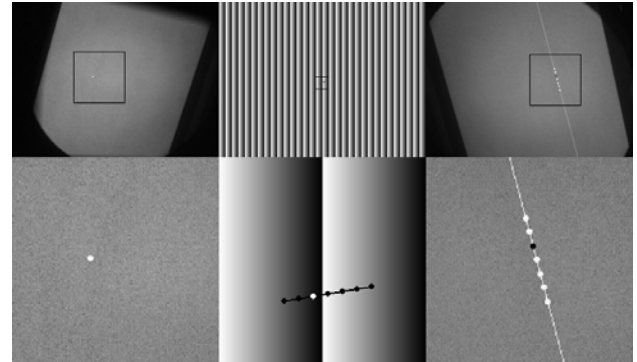


Figure 4: Images of C1 (left), projector (middle), and C2 (right) in the upper row, and image sections (below) representing the unique correspondence because of the short segment length (smaller than one period length) in the projector image

#### 4.3 Technical Realization of Method M2

First a calibration of the considered system must be performed. This will be usually done within an extensive a-priori calibration of the system. The intrinsic and extrinsic camera parameters define the epipolar geometry between the two cameras and the projector. Whereas the intrinsic camera parameters are expected to be constant over a certain time, the extrinsic camera parameters (position and orientation angles) are newly calibrated in every measurement by self calibration (Schreiber and Notni, 2000).

Assume that the calibration procedure is performed and the intrinsic camera parameters are known. The relative orientation between the two cameras and the projector is regarded as fixed. The width of the fringe pattern and the measuring volume must be set. Now all necessary quantities can be calculated applying formulas (1) to (5).

The procedure of finding point correspondences using the method M2 described in section 4.1 is the following. Let us consider one point  $p$  in the image of C1. The corresponding epipolar segment  $s$  in the image of C2 is calculated. The phase values of C2 on  $s$  are determined for a meaningful number of representatives (distance between two points about one pixel).

The candidates  $p'_i$  for correspondence are found by interpolation. Now, for every  $p'_i$  the period number using the reduced Gray-Code sequence is determined which should be unique over the segment  $s$ . Now, the correspondence is found, and the 3D point calculation can be performed as usual.

## 5. EXPERIMENTS AND RESULTS

### 5.1 Experiments

The following experiments were performed in order to evaluate the quality of correspondences (completeness), the measuring accuracy of the 3D points, and the recording time analysis. The results were either compared to measurements with conventional use of two perpendicular projection directions of the fringe patterns denoted by M0 (for accuracy and recording time analysis) and to measurements using full Gray-Code and epipolar geometry (M1) for the comparison of the completeness.

The measuring device “kolibri flex mini” (Notni, 2005) was used. This device has a measuring volume of about 80 mm (diameter) x 25 mm (height). Because the realization of the measuring positions is done by a rotation table for the measuring object, the position of the cameras and the projector may vary on a circle in an approximately constant height. One measuring position was selected. The tilt angle of the cameras was about  $27^\circ$  and of the projector  $22^\circ$ . The measuring distance was between 320 mm ( $d_{min}$ ) and 350 mm ( $d_{max}$ ). The value for  $\lambda_p$  was 0.32 mm (projector pixel size  $20 \mu\text{m} \times 20 \mu\text{m}$ , 16 pixels period length). We selected three measuring objects as shown in Figure 5: a plane surface, a prism, a technical object with a surface of geometric primitives, and a dental object (plaster set of teeth). About 300.000 points were reconstructed for each measuring object.



Figure 5: Measuring objects (prism, machine tool, set of teeth)

The measurements were performed as follows. The intrinsic camera parameters of the projector and the cameras were determined a-priori in a high-precision calibration procedure. A whole body measurement was performed using twelve measuring positions including two tilt angles. A self calibration was performed to get the extrinsic camera parameters. For the analysis one measuring position was selected. The 3D data of the conventional measurement of this position were used for the comparison of the measuring accuracy.

Then the conventionally produced phase images of the selected position were used as input for the epipolar algorithm. For the estimation of the correctness of finding correspondences, the unwrapped phase obtained by using the complete Gray-Code sequence was used. Completeness was tested using the reduced Gray-Code using M2 and the omitted Gray-Code using M3 without resolution of ambiguities. Method M1 was applied in order to get an estimation of the error rate due to the remaining ambiguities. The calculated 3D points were compared to those applying the complete Gray-Code sequence.

Accuracy was determined using the 3D data of the plane. The points obtained using the epipolar constraint were compared to those received by the conventional measurement with two projection directions. Recording time was compared by the number of used images of the sequence distinguishing the use of a four- and a 16-image algorithm for the phase production (Creath, 1986), respectively.

### 5.2 Results

For the completeness analysis a 16-phase algorithm was used. Table 1 shows the percentage rate of completeness compared to full Gray-Code (7 binary images plus light and dark image) use (method M1). The reduced Gray-Code consists of three images according to the given measuring volume and the exterior orientation of the components. The results using method M3 show that the complete omission of the Gray-Code would lead to unacceptable results and needs further improvement. Applying method M4 completeness is almost achieved again.

Object \ Algorithm	M1	M2	M3	M4
Plane	100 %	100 %	98 %	99 %
Prism	100 %	100 %	94 %	98 %
Machine tool	100 %	100 %	77 %	97 %
Set of teeth	100 %	100 %	81 %	98 %

Table 1: Completeness results

The analysis of the accuracy represented by the standard deviation  $\sigma$  of the 3D points to a fitted plane yielded no improvement by the use of the epipolar constraint. The mean value for  $\sigma$  was with  $\sigma = 2.7 \mu\text{m}$  the same as performing the conventional measurement with two projected fringe directions. The biggest difference is to be seen in the image recording time. Table 2 shows the necessary number of images for one sequence and the resulting number of recorded images per sequence for one measuring position.

Algorithm	16-phase	4-phase
Conventional, two directions, full GC	48	24
Full GC with epipolar constraint M1	25	13
Reduced GC M2	21	9
Without GC M3, M5	16	4
Without GC, two directions M4	32	8

Table 2: Results for recording image reduction (GC-Gray-Code)

It can be seen that the number of fringe patterns using the reduced GC as proposed by method M2 can be decreased to 21 or 9 images without limitation of the accuracy and the completeness using the 16- or 4-phase-algorithm, respectively.

## 6. DISCUSSION AND OUTLOOK

The results show that a considerable speed-up of the recording time can be achieved without loss of accuracy using method M2. If the ambiguity problem can be solved a further reduction of the recording time is possible. The epipolar constraint, directly replace a part of the Gray-Code so that no influence on the calculated 3D points occurs.

However the replacement of the conventional implementation in measuring devices brings some other problems which should not be neglected. First, the new algorithm requires some more calculation time. It was not yet analyzed practically how much

more this is. It should be performed in the next months. Second, phase images are usually applied by filtering operators. These operators are mainly designed for unwrapped phase images. This means that all concerning operators must be converted. This may also increase the calculation time.

In principal, algorithms with shorter image recording time are more convenient for applications with moving objects or a moving sensor or other time limiting reasons. Hence the method should be implemented in some existing 3D measuring systems, as e.g. the intraoral scanner (Kühmstedt et al., 2007b) and the “kolibri cordless” (Munkelt et al., 2007) system. Future work should include the conversion of the filtering operators to unwrapped phase images and the performance of further tests and experiments.

Another task for future work is the realization of unambiguousness when the binary code sequence is totally omitted. As it was already shown in this work, the measuring system can be designed for full omission of the Gray-Code sequence, when the measuring distance is not very extended. This result will lead to a considerable speed-up of recording and measurement time of such systems. For arbitrary measuring distances it will be a sophisticated task to design a system without use of the Gray-Code, because the triangulation angle between the projector and camera C1 becomes very small, typically about or less than 1°. However, this problem should be also solved within our future work.

## REFERENCES

Albrecht, P. and Michaelis, B., 1997. Improvement of the spatial resolution of an optical 3-D measurement procedure. IEEE Instr. and Measurement Technology Conference (IMTC/97), Ottawa, Canada, pp. 158-162

Battle J., Mouaddib, E., and Salvi, J., 1998. Recent progress in coded structured light as a technique to solve the correspondence problem: a survey. PR, Vol. 31, No 7, pp 963-982

Bräuer-Burchardt C., Munkelt C., Heinze M., Kühmstedt P., and Notni G., 2008. Phase unwrapping in fringe projection systems using epipolar geometry. Advanced Concepts for Intelligent Vision Systems, pp. 422-432

Bräuer-Burchardt, C., 2005. A new methodology for determination and correction of lens distortion in 3D measuring systems using fringe projection. In Pattern Recognition (Proc 27th DAGM), Springer LNCS, pp. 200-207

Creath, K., 1986. Comparison of phase-measurement algorithms, surface characterization and testing. Proc. SPIE 680, pp. 19-28

Ishiyama, R., Okatani, T., Deguchi, K., 2007a. Precise 3-d measurement using uncalibrated pattern projection. Proc. IEEE Int. Conf. on Image Proc. (ICIP), vol. 1, pp. 225-228

Ishiyama, R., Sakamoto, S., Tajima, J., Okatani, T., and Deguchi, K., 2007b. Absolute phase measurements using geometric constraints between multiple cameras and projectors. Applied Optics, Vol. 46, Issue 17, pp. 3528-3538

Young, M., Beeson, E., Davis, J., Rusinkiewicz, S., Ramamoorthi, R., 2007. Viewpoint-coded structured light. Proc. CVPR, pp. 1-8

Kühmstedt, P., Munkelt, C., Heinze, M., Himmelreich, M., Bräuer-Burchardt, C., Notni, G., 2007a. 3D shape measurement with phase correlation based fringe projection. Proc. SPIE vol. 6616, pp. 66160 B-1 - B-9

Kühmstedt, P., Bräuer-Burchardt, C., Munkelt, C., Heinze, M., Palme, M., Schmidt, I., Hintersehr, J., Notni, G., 2007b. Intraoral 3D scanner, Proc SPIE Vol. 6762, pp. 67620E-1 - 67620E-9

Li, Z., Shi, Y., and Wang, C., 2009. Real-time complex object 3D measurement. Proc. ICCMS, pp. 191-194

Luhmann, T., Robson, S., Kyle, S., Harley, I., 2006. Close range photogrammetry. Wiley Whittles Publishing

Maas, H.-G., 1992. Robust automatic surface reconstruction with structured light. IAPRS, Vol. XXIX, Part B5, pp. 709-713

Malz, R., 1989. Adaptive light encoding for 3-D sensing with maximum measurement efficiency. In Proc. 11th DAGM-Symposium, Hamburg, Germany. Informatik-Fachberichte Vol. 219, pp. 98-105

Munkelt, C., Bräuer-Burchardt, C., Kühmstedt, P., Schmidt, I., Notni, G., 2007. Cordless hand-held optical 3D sensor. Proc. SPIE Vol. 6618, pp. 66180D-1

Notni, G., Kühmstedt, P., Heinze, M., Munkelt, C., Himmelreich, M., 2005. Selfcalibrating fringe projection setups for industrial use. Proc Finge 2005, Springer, pp. 436-441

Robin E. and Valle, V., 2004. Phase demodulation from a single fringe pattern based on a correlation technique. Appl. Opt. 43, pp. 4355-4361

Sansoni G., Carocci M., and Rodella R., 1999. Three-dimensional vision based on a combination of Gray-Code and phase-shift light projection: analysis and compensation of the systematic errors. Applied Optics, Vol. 38, Issue 31, pp. 6565-6573

Schreiber, W. and Notni, G., 2000. Theory and arrangements of self-calibrating whole-body three-dimensional measurement systems using fringe projection technique. Opt. Eng. 39, pp. 159-169

Wiegmann, A., Wagner, H., Kowarschik, R., 2006. Human face measurement by projecting bandlimited random patterns. Optics Express 7692, Vol. 14, No 17, pp. 7692 - 7698

Zhang, H., Lalor, M.J., and Burton, D.R., 1999. Spatiotemporal phase unwrapping for the measurement of discontinuous objects. In dynamic fringe-projection phase-shifting profilometry. Applied Optics. 38, pp. 3534-3541

Zhang S. and Yau, S.T., 2006. High-resolution, real-time 3D absolute coordinate measurement based on a phase-shifting method. Optics Express, Vol. 14, Issue 7, pp. 2644-2649